Fabrication of Chitosan Nanoparticles with Aggregation-Induced Emission Characteristics and Their Applications in Long-Term Live Cell Imaging

Min Li, Yuning Hong, Zhengke Wang, Sijie Chen, Meng Gao, Ryan T. K. Kwok, Wei Qin, Jacky W. Y. Lam, Qichang Zheng,* Ben Zhong Tang*

Chitosan with tetraphenylethene pendants (TPE-CS) are synthesized by reaction between amine and isothiocyanate groups of chitosan and tetraphenylethene (TPE), respectively. Nanoparticles of TPE-CS (TPE-CS NPs) are fabricated by ionic gelation method. The NPs are uniform in size, spherical in shape, monodispersed, and positive in surface charge. The suspension of TPE-CS NPs emits strong blue fluorescence under photoexcitation due to the aggregation-induced emission characteristics of the TPE moieties. The NPs can be internalized into cytoplasm through endocytosis pathway and retain inside the live cells to image the cells. Cytotoxicity assay reveals that TPE-CS NPs are cytocompatible and thus can be used for long-term live cell imaging.

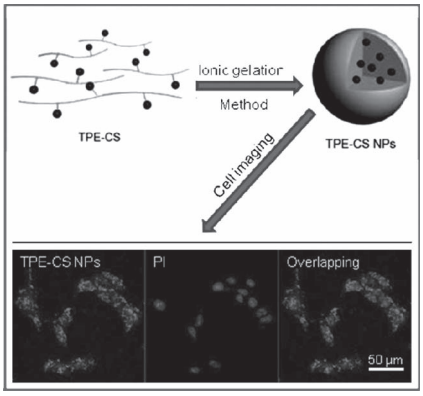

M. Li, Q. Zheng
Department of Hepatobiliary Surgery, Union Hospital, Tongji Medical College, Huazhong University of Science and Technology, Wuhan 430022, China
E-mail: qc_zheng@mail.hust.edu.cn
M. Li, Y. Hong, Z. Wang, S. Chen, M. Gao, R. T. K. Kwok, W. Qin, J. W. Y. Lam, B. Z. Tang
Department of Chemistry, Institute for Advanced Study, State Key Laboratory of Molecular Neuroscience, Institute of Molecular Functional Materials and Division of Biomedical Engineering, The Hong Kong University of Science and Technology, Clear Water Bay, Kowloon, Hong Kong, China
E-mail: tangbenz@ust.hk
B. Z. Tang
Guangdong Innovative Research Team, SCUT-HKUST Joint Research Laboratory, State Key Laboratory of Luminescent Materials and Devices, South China University of Technology, Guangzhou 510640, China
B. Z. Tang
HKUST Shenzhen Research Institute, No. 9 Yuexing 1st RD, South Area, Hi-tech Park, Nanshan, Shenzhen 518057, China

1. Introduction

Fluorescence imaging has emerged as an important modality for studying biological and biochemical processes with spatial and temporal resolution.[1] The crossover of nanotechnology and fluorescence imaging in recent years has bolstered the progress in a variety of areas in particular early-stage cancer diagnosis, tracking drug, or gene delivery vehicles, and monitoring cancer treatment.[2] Typical nanomaterials for fluorescence imaging include fluorescent organic nanoparticles (NPs) and inorganic semiconductor quantum dots (QDs). QDs are highly luminescent and resistant to photobleaching and have been commonly used for cell labeling and imaging.[3] The in vivo application of QDs, however, has been limited because of their inherent toxicity from the heavy metal constituents.[3,4] For example, Ye et al.[5] have recently reported that most cadmium from initial QDs accumulates in the liver, spleen, and kidneys of the rhesus macaques for 3 months

DOI: 10.1002/marc.201200760

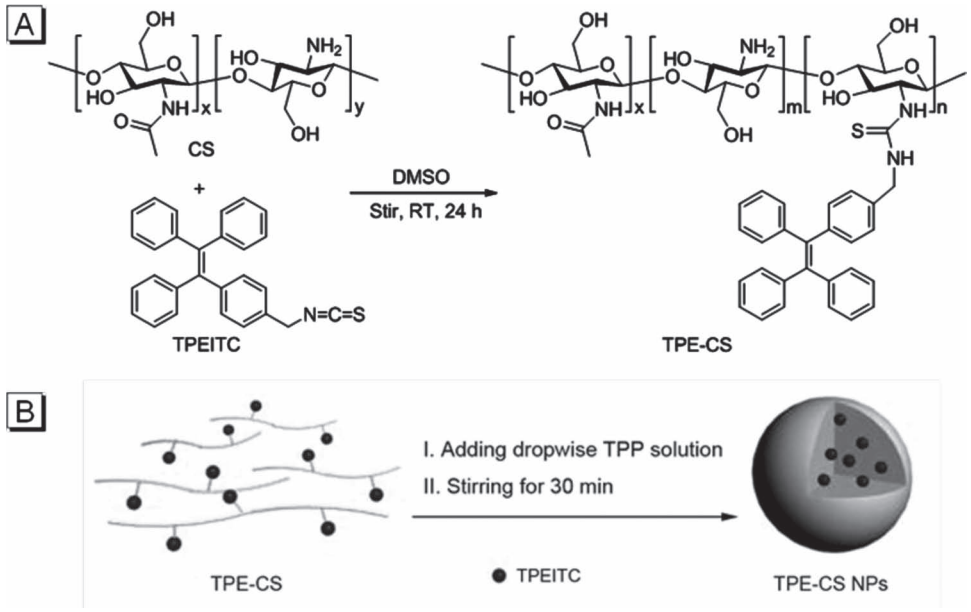

Scheme 1. (A) Synthetic route of TPE-CS and (B) schematic illustration of the fabrication of TPE-CS NPs by ionic gelation method.

after intravenous injection. Therefore, the development of new class of fluorescent NPs with improved biocompatibility, photostability, and biodegradability is an imperative task for NPs to be employed for in vitro long-term live cell tracking and in vivo cancer imaging.

Chitosan (CS), a linear polysaccharide consisting of *N*-acetyl-glucosamine (acetylated) and glucosamine (deacetylated) repeating units, is non-toxic, biodegradable, and non-immunogenic, representing an ideal material for biomedical applications.[2b,6] CS can be easily modified through chemical reaction because of its abundant reactive amine and hydroxyl groups on the backbone.[7] Through functionalization, CS NPs can be used as a carrier for the delivery of antitumor drugs[8] and genes.[9] Fluorescent agents are covalently attached to CS and the resultant materials can be applied as reporters for imaging, tracing, and analysis.[2b,10] However, light emission from CS NPs is rather weak due to the emission quenching caused by the aggregation of fluorophores in the solid state.[11] Aggregation of the conventional fluorophores normally decreases the light emission because of the strong intermolecular π–π stacking interactions, which promote the formation of detrimental species such as excimers or exciplexes.[12]

To overcome this problem, fluorescent agents with aggregation-induced emission (AIE) characteristics are used to label CS. Propeller-like molecules, such as hexaphenylsilole and tetraphenylethene (TPE), are nonemissive in solution but induced to emit efficiently by aggregation formation.[12,13] Restriction of intramolecular motion (RIM) is proposed to be the main cause for the AIE effect.[12,14] Previously, we have successfully fabricated strongly fluorescent silica NPs hybridized with AIE molecules and explored their applications for cell imaging.[15] The silica NPs, however, are not biodegradable. Herein, we report the synthesis of TPE conjugated CS (TPE-CS) and the sequent fabrication of TPE-CS NPs by using ionic gelation method. The NPs exhibit strong fluorescence and low cytotoxicity, making them well suited for cell imaging. The investigation of endocytosis and exocytosis processes of the NPs shows that these NPs can retain inside live cells for a long period of time, thus enabling long-term cell imaging and tracking.

2. Results and Discussion

2.1. Preparation and Characterization of TPE-CS NPs

TPE-CS was synthesized by addition reaction between the primary amines on CS and the isothiocyanate group on TPEITC (Scheme 1A). The product was characterized by ^{1}H NMR and FTIR from which satisfactory analysis data were obtained. The new peaks present at the aromatic region of the ^{1}H NMR spectra with chemical shift around 7.22–7.17 ppm indicate the conjugation of TPEITC to the CS skeleton (Figure S1, Supporting Information). According to the peak integrals of the aromatic units of TPE and the carbohydrate of CS, the substitution degree of TPE is calculated to be 4.13% (molar ratio). The disappearance of the isothiocyanate bond (N=C=S) characteristic peak at 2045 cm^{-1} in the FTIR spectrum further supports the successful conjugation of TPE to CS in the product (Figure S2, Supporting Information).

Nanoparticles of TPE-CS were fabricated by using ionic gelation method (Scheme 1B). TPE-CS was dissolved in

acetic acid aqueous solution to form the cationic amino groups and then into the solution was dropwisely added sodium tripolyphosphate (TPP) solution under constant stirring. The TPE-CS NPs were formed through the inter- and intrachain crosslinking of the positively charged amino groups of CS and the negatively charged phosphate groups of TPP.[8,16] This method is simple and under mild condition while avoiding the use of toxic cross-linking agent such as glutaraldehyde.[8]

Analysis by dynamic light scattering (DLS) reveals the average hydrodynamic diameter of TPE-CS NPs is 170 nm with a small polydispersity of 0.13 (Figure S3A, Supporting Information). Under transmission electron microscope (TEM), we found that TPE-CS NPs are monodispersed with spherical shapes (Figure S3B, Supporting Information). The particle sizes are smaller than that measured by DLS owing to the shrinkage of the NPs under high vacuum in the TEM chamber. Thanks to the abundant amino groups on the CS backbones, the surface of TPE-CS NPs is positively charged when the pH of the solution is up to 7.0 from zeta potential analysis (Figure S4, Supporting Information). Such property may facilitate the uptake and internalization of the TPE-CS NPs to cells.

2.2. Light Emission

Photoluminescence (PL) spectra of TPE-CS NPs, TPE-CS, and CS NPs were measured in 1% acetic acid aqueous solution (adjusted to pH 2.5). TPE-CS is faintly fluorescent when dissolved in acidic solution while the suspension of TPE-CS NPs is strongly emissive (Figure 1A). At low pH, TPE-CS is water soluble and the TPE pendants can enjoy intramolecular motions, which lead to weak fluorescence according to the AIE principle. The intramolecular motions are impeded when TPE-CS is fabricated into NPs, or when the pH is adjusted to 7.0 where TPE-CS is no longer soluble (Figure 1B). At pH 7.0, the PL intensity of TPE-CS NPs is also increased due to the shrink of the NPs. Without the TPE units, CS NPs are nonemissive at either pH 2.5 or 7.0. The differences in PL intensity can be clearly observed under UV illumination as shown in the photographs of Figure 1 and S5 (Supporting Information).

2.3. Cytotoxicity

To evaluate the biocompatibility of TPE-CS NPs as a live cell imaging agent, the cytotoxicity was investigated using 3-(4,5-dimethylthiazol-2-yl)-2,5- diphenyltetrazolium bromide (MTT) assay. MTT can reflect the mitochondrial activity of cells and represent a parameter for their metabolic activity. As shown in Figure 2A, the cytotoxicity of NPs is dose-dependent after exposure to cells for 24 h. The viability is 90.42%, 87.72%, and 84.25% at the concentration of 25, 50, and 75 μg mL^{-1}, respectively, indicating TPE-CS NPs are highly biocompatible for live cell imaging.

2.3. Cell Imaging

Owing to the AIE property, the PL intensity of TPE-CS NPs is increased along with the increase of the NPs concentration (Figure S6A, Supporting Information). With the increase of NPs concentration, the fluorescent intensity of live HeLa cells stained with TPE-CS NPs is enhanced (Figure S6B, Supporting Information), clearly indicating the degree of TPE-CS NPs uptake is dose dependent. Based on the above results, the dose of 50 μg mL^{-1} is chosen for the following experiments. The three-dimensional (3D) confocal image of HeLa cells stained with TPE-CS NPs revealed that the NPs are mainly localized in the cytoplasm surrounding the cell nucleus (blue: TPE-CS NPs; red: PI labeling in Figure S7, Supporting Information).

Photostability is a critical parameter for cell imaging and tracking. The photostability of TPE-CS NPs are assessed by using confocal laser scanning microscopy. As shown in Figure S8 (Supporting Information), the PL intensity of TPE-CS NPs stained cells is kept 77.7% of the original signal even under continuous excitation at 405 nm (power at 0.6 mW) for 30 min. Such superior photostability prompts us to further investigate their use for long-term cell imaging.

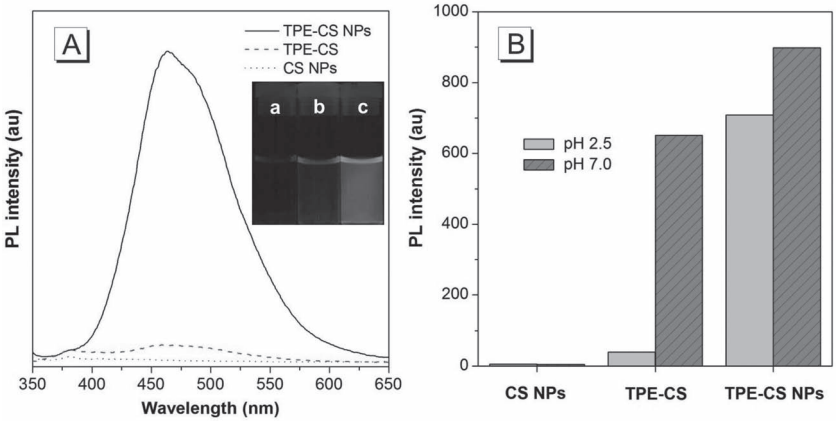

Figure 1. (A) PL spectra of TPE-CS NPs, TPE-CS, and CS NPs in 1% acetic acid aqueous solutions at pH 2.5. Inset: photograph of (a) CS NPs, (b) TPE-CS, and (c) TPE-CS NPs taken under 365 nm UV illumination of a hand held UV lamp. (B) Histogram of relative PL intensity at 465 nm of CS NPs, TPE-CS, and TPE-CS NPs in an aqueous solution with different pH. Concentration: 0.2 mg mL^{-1}; excitation wavelength: 338 nm.

2.4. Cellular Uptake and Exocytosis

It is known that NPs are mainly internalized by cells through endocytosis pathway,[17] which is an

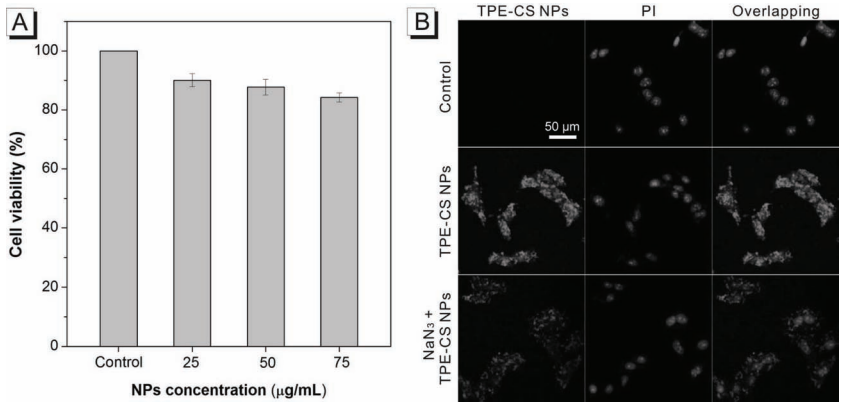

Figure 2. (A) Cytotoxicity of TPE-CS NPs on HeLa cells evaluated by MTT assay. (B) Confocal images of HeLa cells in the absence or presence of 0.1% sodium azide (NaN_3) in serum-free culture medium for 1 h before incubation with 50 μg mL^{-1} TPE-CS NPs for 2 h.

energy-dependent process. To testify whether TPE-CS NPs are using the same manners, HeLa cells were pretreated with 0.1% NaN_3, an endocytosis inhibitor, prior to the incubation with TPE-CS NPs. Confocal images demonstrate that the fluorescence of the cells treated with NaN_3 is weaker than that of the cells in the absence of endocytosis inhibitor (Figure 2B). Similar result was obtained by quantitative analysis using flow cytometry (Figure S9, Supporting Information). The fluorescence of NaN_3-treated cells shifts to the lower intensity as compared with the untreated ones. NaN_3 is reported to reduce the cellular synthesis of ATP, the energy currency, and thus inhibit the endocytosis process. However, endocytosis is not completely suppressed owing to the presence of exogenous ATP and glucose in the serum-free medium.[18] All these data support that the uptake of the TPE-CS NPs are mainly through endocytosis pathway.

On the other hand, exocytosis may occur as well as endocytosis when the cells are exposed to NPs.[19] Scattered fluorescence from TPE-CS NPs in 3T3 cells is observed when the cells are co-cultured with the prestained HeLa cells for 24 h (Figure S10, Supporting Information), suggesting that small amount of NPs is excreted from the HeLa cells after their internalization into the cytoplasm.

2.5. Long-Term Cell Tracking

In our previous work, an AIE-active cytophilic silole derivative was reported to track live cells for 4 passages (Psg), which is superior to the commercial dye MitoTracker Green FM.[20] However, cell tracking in a longer period is expected for practical use. TPE-CS NPs have good biocompatibility and low exocytosis and we thus examined their application for long-term cell tracking.

The cells were first incubated with the NPs for 24 h and rinsed with phosphate buffer to remove excess amount of NPs. Image was taken and referred to as the 1st Psg. Compared to shorter incubation time such as 4 h, the fluorescence intensity at the 1st Psg is much stronger (Figure 3), suggesting that longer incubation time may enable more TPE-CS NPs to enter into the cells. One third of the cells from the 1st Psg were subcultured into another dish for continual tracking. Upon additional 24 h incubation in fresh growth medium, another image was taken and referred to the 2nd Psg. This step was repeated every 24 h with the increase of Psg number. As shown in Figure 3, although the fluorescence from daughter cells is decreased, TPE-CS NPs are able to trace the living cells for 7 Psg, a period more than 160 h. The weakening of fluorescence intensity may attribute to the decrease of NPs/cells ratio during cell division.

3. Conclusions

In summary, TPE conjugated CS nanoparticles (TPE-CS NPs) were successfully fabricated by ionic gelation method. These NPs are monodispersed and uniform in size with narrow size distribution. Owing to the RIMs of the TPE

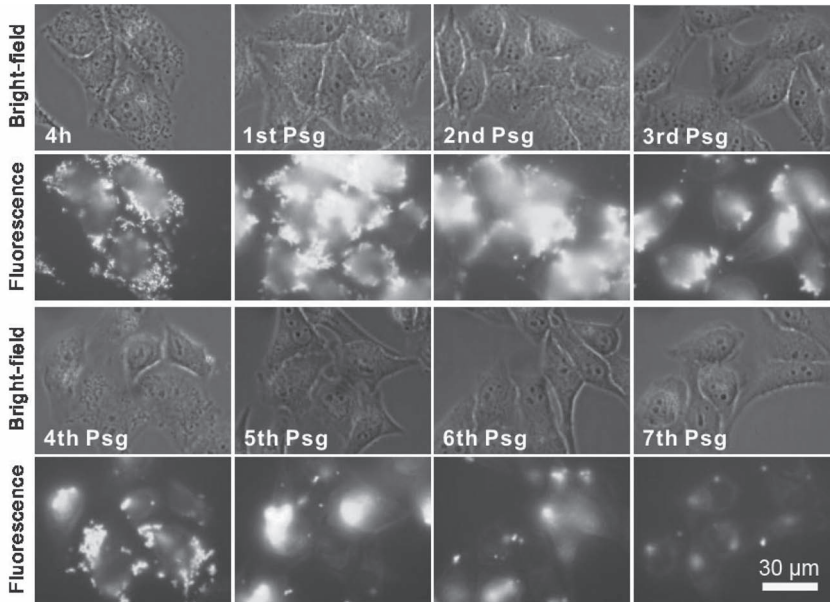

Figure 3. Long-term tracking of HeLa cells from 4 h to 7 days. Bright-field and fluorescence of HeLa cells stained with 50 μg mL^{-1} TPE-CTS NPs. Exposure time = 500 ms.

moieties in the NPs architecture, TPE-CS NPs emit bright blue fluorescence. MTT assay suggests that the NPs are of low cytotoxicity to HeLa cells. The NPs can stain live cells through energy-dependent endocytosis. Once enter the cells, the NPs can retain in the cells and thus enable long-term tracking of 7 Psg of cell growth. Moreover, the NPs are photostable with less than 25% signal loss upon continuous excitation under fluorescence microscope for 30 min. All these incredible features render the AIE-active, strongly fluorescent, photostable, and biocompatible TPE-CS NPs as promising materials for long-term live cell imaging and monitoring of drug or gene delivery.

Supporting Information

Supporting Information is available from the Wiley Online Library or from the author.

Acknowledgements: The work reported in this paper was partially supported by the National Basic Research Program of China (973 Program; 2013CB834701), the National Science Foundation of China (20974028), the RPC and SRFI Grants of HKUST (RPC10SC13, RPC11SC09 and SRFI11SC03PG), the Research Grants Council of Hong Kong (604711, 602212, HKUST2/CRF/10 and N_HKUST620/11), the Innovation and Technology Commission (ITCPD/17-9), and the University Grants Committee of Hong Kong (AoE/P-03/08). B. Z. Tang thanks the support of the Guangdong Innovative Research Team Program of China (201101C0105067115).

Received: November 27, 2012; Revised: January 16, 2013; Published online: February 11, 2013; DOI: 10.1002/marc.201200760

Keywords: aggregation-induced emission; cell imaging; chitosan; nanoparticles; tetraphenylethylene

[1] a) R. M. Hoffman, *Nat. Rev. Cancer* **2005**, *5*, 796; b) D. A. Christian, O. B. Garbuzenko, T. Minko, D. E. Discher, *Macromol. Rapid Commun.* **2010**, *31*, 135; c) Y. Hong, M. Haussler, J. W. Y. Lam, Z. Li, K. K. Sin, Y. Dong, H. Tong, J. Liu, A. Qin, R. Renneberg, B. Z. Tang, *Chem. Eur. J.* **2008**, *14*, 6428; d) H. Shi, R. T. K. Kwok, J. Liu, B. Xing, B. Z. Tang, B. Liu, *J. Am. Chem. Soc.* **2012**, *134*, 17972.

[2] a) K. Li, Y. Jiang, D. Ding, X. Zhang, Y. Liu, J. Hua, S. S. Feng, B. Liu, *Chem. Commun.* **2011**, *47*, 7323; b) P. Agrawal, G. J. Strijkers, K. Nicolay, *Adv. Drug Delivery Rev.* **2010**, *62*, 42; c) W. Qin, D. Ding, J. Liu, W. Z. Yuan, Y. Hu, B. Liu, B. Z. Tang, *Adv. Funct. Mater.* **2012**, *22*, 771; d) I. K. Park, K. Singha, R. B. Arote, Y. J. Choi, W. J. Kim, C. S. Cho, *Macromol. Rapid Commun.* **2010**, *31*, 1122.

[3] X. Michalet, F. F. Pinaud, L. A. Bentolila, J. M. Tsay, S. Doose, J. J. Li, G. Sundaresan, A. M. Wu, S. S. Gambhir, S. Weiss, *Science* **2005**, *307*, 538.

[4] S. J. Cho, D. Maysinger, M. Jain, B. Roder, S. Hackbarth, F. M. Winnik, *Langmuir* **2007**, *23*, 1974.

[5] L. Ye, K. T. Yong, L. Liu, I. Roy, R. Hu, J. Zhu, H. Cai, W. C. Law, J. Liu, K. Wang, Y. Liu, Y. Hu, X. Zhang, M. T. Swihart, P. N. Prasad, *Nat. Nanotechnol.* **2012**, *7*, 453.

[6] T. Kean, M. Thanou, *Adv. Drug Delivery Rev.* **2010**, *62*, 3.

[7] H. Chen, M. Li, T. Wan, Q. Zheng, M. Cheng, S. Huang, Y. Wang, *J. Mater. Sci. Mater. Med.* **2012**, *23*, 431.

[8] S. A. Agnihotri, N. N. Mallikarjuna, T. M. Aminabhavi, *J. Controlled Release* **2004**, *100*, 5.

[9] T. Kean, S. Roth, M. Thanou, *J. Controlled Release* **2005**, *103*, 643.

[10] J. H. Na, H. Koo, S. Lee, K. H. Min, K. Park, H. Yoo, S. H. Lee, J. H. Park, I. C. Kwon, S. Y. Jeong, K. Kim, *Biomaterials* **2011**, *32*, 5252.

[11] H. Mok, H. Jeong, S. J. Kim, B. H. Chung, *Chem. Commun.* **2012**, *48*, 8628.

[12] a) Y. Hong, J. W. Y. Lam, B. Z. Tang, *Chem. Soc. Rev.* **2011**, *40*, 5361; b) Y. Hong, J. W. Y. Lam, B. Z. Tang, *Chem. Commun.* **2009**, 4332.

[13] a) J. Luo, Z. Xie, J. W. Lam, L. Cheng, H. Chen, C. Qiu, H. S. Kwok, X. Zhan, Y. Liu, D. Zhu, B. Z. Tang, *Chem. Commun.* **2001**, 1740; b) T. Wang, Y. Cai, Z. Wang, E. Guan, D. Yu, A. Qin, J. Sun, B. Z. Tang, C. Gao, *Macromol. Rapid Commun.* **2012**, *33*, 1584.

[14] J. Shi, N. Chang, C. Li, J. Mei, C. Deng, X. Luo, Z. Liu, Z. Bo, Y. Q. Dong, B. Z. Tang, *Chem. Commun.* **2012**, *48*, 10675.

[15] a) M. Faisal, Y. Hong, J. Liu, Y. Yu, J. W. Y. Lam, A. Qin, P. Lu, B. Z. Tang, *Chem. Eur. J.* **2010**, *16*, 4266; b) F. Mahtab, Y. Yu, J. W. Y. Lam, J. Liu, B. Zhang, P. Lu, X. Zhang, B. Z. Tang, *Adv. Funct. Mater.* **2011**, *21*, 1733; c) M. Li, J. W. Y. Lam, F. Mahtab, S. Chen, W. Zhang, Y. Hong, J. Xiong, Q. Zheng, B. Z. Tang, *J. Mater. Chem. B* **2013**, *1*, 676.

[16] H. Zhang, M. Oh, C. Allen, E. Kumacheva, *Biomacromolecules* **2004**, *5*, 2461.

[17] H. Hillaireau, P. Couvreur, *Cell Mol. Life Sci.* **2009**, *66*, 28736.

[18] H. Yang, C. Lou, M. Xu, C. Wu, H. Miyoshi, Y. Liu, *Int. J. Nanomed.* **2011**, *6*, 2023.

[19] Z. Chu, Y. Huang, Q. Tao, Q. Li, *Nanoscale* **2011**, *3*, 3291.

[20] Y. Yu, C. Feng, Y. Hong, J. Liu, S. Chen, K. M. Ng, K. Q. Luo, B. Z. Tang, *Adv. Mater.* **2011**, *23*, 3298.